Industrial Robot Trajectory Stiffness Mapping for Hybrid Manufacturing Process

Zhiyuan Wang[*], Renwei Liu, Xueyang Chen, Todd Sparks and Frank Liou

Department of Mechanical and Aerospace Engineering, Missouri University of Science and Technology, Rolla, MO, 65409

Abstract: The application of using industrial robots in hybrid manufacturing is promising, but the heavy external load applied on robot system, including the weight of deposition extruder or the cutting force from machining process, affects the operation accuracy significantly. This paper proposed a new method for helping robot to find the best position and orientation to perform heavy duty tasks based on the current system stiffness. By analyzing the robot kinematic and stiffness matrix properties of robot, a new evaluation formulation has been established for mapping the trajectory's stiffness within the robot's working volumetric. The influence of different position and orientation for hybrid manufacturing working path in different scale has been discussed. Finally, a visualized evaluation map can be obtained to describe the stiffness difference of a robotic deposition working path at different positions and orientations. The method is important for improving the operation performance of robot system with current stiffness capability.

Keywords: Industrial robot, robot stiffness, jacobian matrix, hybrid manufacturing.

1. INTRODUCTION

Serial industrial robots are mainly used in industry for tasks that require good repeatability but not necessarily good global position and orientation accuracy of the robot end effector. For example, these robots are generally used for pick and place, painting and welding operations. These kind of tasks do not apply much external load or force on the robot system, the stiffness of robot system itself is sufficient to satisfy these operations' accuracy requirements. With the development of automation technology, the scope of applications using industrial robots is getting wider and wider. The potential applications of industrial robots in hybrid manufacturing, which usually involve both robot deposition process and robot machining process, have been gaining worldwide attention from researchers. But the external load from hybrid manufacturing process applied on robot system, including the weight of fused pellets extruder for deposition process and the cutting force from metal machining process, is much larger than common tasks for robot. Thus, to perform these operations, the robots must show good kinematic and elastostatic performance.

Some research works discuss the following: (i) tool path optimization considering both kinematic and dynamic robot performance [1-4]; (ii) the determination of optimal cutting parameters to avoid tool chattering [5-7]; (iii) robot stiffness analysis [8]; and (iv) the determination of robot performance indices [9-12].

Robot stiffness is also a relevant performance index for robot machining [13]. Accordingly, this paper discusses the stiffness modeling of serial robots and identifies their stiffness parameters. Some stiffness models can be found in the literature for serial and parallel manipulators [14-15]; however, the identification of stiffness parameters has yet to be determined. Two methods were presented by Abele *et al*. [16] to obtain the Cartesian stiffness matrix (CaSM) of a five-revolute robot. The first method consists of clamping all of the joints except one to measure its stiffness. The second method measures the displacements of the robot end-effector due to certain applied loads and evaluates the robot Cartesian stiffness matrix throughout its Cartesian workspace with some interpolations.

In addition to the study of dynamic stiffness (which is useful for vibration and stability problems), the study of robot rigidity can be performed through the analysis of static stiffness maps. Static stiffness maps can be used to assess the level of positioning error for a given production task, i.e., for a given type of loading condition [17-19]. They can also be used to compare different architectures or configurations. A few studies in the literature provide the stiffness maps of industrial robots. Using the virtual joint method, Gosselin [20] provided stiffness maps with the aim of setting a tool for the computer-aided design of a planar 3-DOF parallel manipulator and a spatial 6-DOF parallel manipulator. Majou *et al*. [21] identified the stiffest areas in the workspace of the Orthoglide, which is a three-axis translational parallel kinematic machine, by analyzing its stiffness maps for a specific machining

*Address correspondence to this author at the Department of Mechanical and Aerospace Engineering, Missouri University of Science and Technology, Rolla, MO, 65409; Tel: +1-573-612-8669; E-mail: zwc4b@mst.edu

task. Ruggiu [22] mapped the stiffness of a translational parallel mechanism using a general formulation based on the development of the principle of virtual work. Pinto *et al*. [23] used MSA, finite element method (FEM), and experimental measurements for the stiffness mapping of a Daedalus I, and concluded that volume FEM was more precise but leads to long calculation times.

The research objects of the above studies focus on robot stiffness parameter identification or stiffness distribution in robot working volume. This paper provides a new concept of viewing robot stiffness mapping problem, this method takes the turning points of working path into consideration, by analyzing robot kinematic and the property of robot cartesian stiffness matrix, establish an evaluation formualtion to describe the difference of trajectory stiffness at different position and orientation. The paper will first introduce the mathematics foundation of robot jacobian matrix and how solve the jacobian matrix for a 6 DOF industrial robot, then based on two reasonable assumptions establish the stiffness model of serial manipulator and trajectory stiffness evaluation formualtion, finally apply the proposed method on a specific typical zigzag working path, find out the best position and orientation to perform this in the robot working volume and discuss how the size of working path affect the stiffness mapping analysis.

2. KINEMATIC JACOBIAN OF ROBOT

The Jacobian matrix is the matrix of all first-order partial derivatives of a vector-valued function. Suppose there are following multivariate functions:

$$
\begin{cases}
y_1 = f_1(x_1, x_2, x_3, x_4, x_5, x_6) \\
y_2 = f_2(x_1, x_2, x_3, x_4, x_5, x_6) \\
y_3 = f_3(x_1, x_2, x_3, x_4, x_5, x_6) \\
y_4 = f_4(x_1, x_2, x_3, x_4, x_5, x_6) \\
y_5 = f_5(x_1, x_2, x_3, x_4, x_5, x_6) \\
y_6 = f_6(x_1, x_2, x_3, x_4, x_5, x_6)
\end{cases}
\tag{1}
$$

$x_1 ... x_6$ are the independent variables of f_i, y_i is the dependent variable of f_i. It can be written in vector form as:

$$Y = F(X) \tag{2}$$

The multiple variables' first derivative of functions can be solved from equation (2.1):

$$
\begin{cases}
dy_1 = \frac{\partial f_1}{\partial x_1} dx_1 + \frac{\partial f_1}{\partial x_2} dx_2 \cdots + \frac{\partial f_1}{\partial x_6} dx_6 \\
dy_2 = \frac{\partial f_2}{\partial x_1} dx_1 + \frac{\partial f_2}{\partial x_2} dx_2 \cdots + \frac{\partial f_2}{\partial x_6} dx_6 \\
dy_3 = \frac{\partial f_3}{\partial x_1} dx_1 + \frac{\partial f_3}{\partial x_2} dx_2 \cdots + \frac{\partial f_3}{\partial x_6} dx_6 \\
dy_4 = \frac{\partial f_4}{\partial x_1} dx_1 + \frac{\partial f_4}{\partial x_2} dx_2 \cdots + \frac{\partial f_4}{\partial x_6} dx_6 \\
dy_5 = \frac{\partial f_5}{\partial x_1} dx_1 + \frac{\partial f_5}{\partial x_2} dx_2 \cdots + \frac{\partial f_5}{\partial x_6} dx_6 \\
dy_6 = \frac{\partial f_6}{\partial x_1} dx_1 + \frac{\partial f_6}{\partial x_2} dx_2 \cdots + \frac{\partial f_6}{\partial x_6} dx_6
\end{cases}
\tag{3}
$$

It can be written in vector form as:

$$dY = \frac{\partial F}{\partial X} dX \tag{4}$$

Make $J = \frac{\partial F}{\partial X}$, thus J is the jacobian matrix to illustrate the mapping relationship between dY and dX:

$$\dot{Y} = J(X)\dot{X} \tag{5}$$

Assume the movement function of robot is:

$$x = x(q) \tag{6}$$

x is the vector representing the position and orientation of robot's end effector, q is the vector representing the angle value of each joint. From equation (2.5), the jacobian matrix of robot $J(q)$ is:

$$\dot{x} = J(q)\dot{q} \tag{7}$$

Or it can be written in matrix form as:

$$
\begin{bmatrix} dx \\ dy \\ dz \\ \delta x \\ \delta y \\ \delta z \end{bmatrix}
=
\begin{bmatrix} Robot \\ Jacobian \end{bmatrix}
\begin{bmatrix} d\theta_1 \\ d\theta_2 \\ d\theta_3 \\ d\theta_4 \\ d\theta_5 \\ d\theta_6 \end{bmatrix}
\tag{8}
$$

3. SOLVE THE JACOBIAN MATRIX OF ROBOT

The Nachi Robot (SC300F-02) is used as an illustrate example throughout this paper. It has a 4.1 m^2 (cross-section area) operating area and a $300°$ rotation range for the base motor (Figure **1**), which could provide a much bigger working envelope than any current hybrid manufacturing system. The 6-axis movement mechanism makes the deposition/machining process more flexible in building a model with complex features.
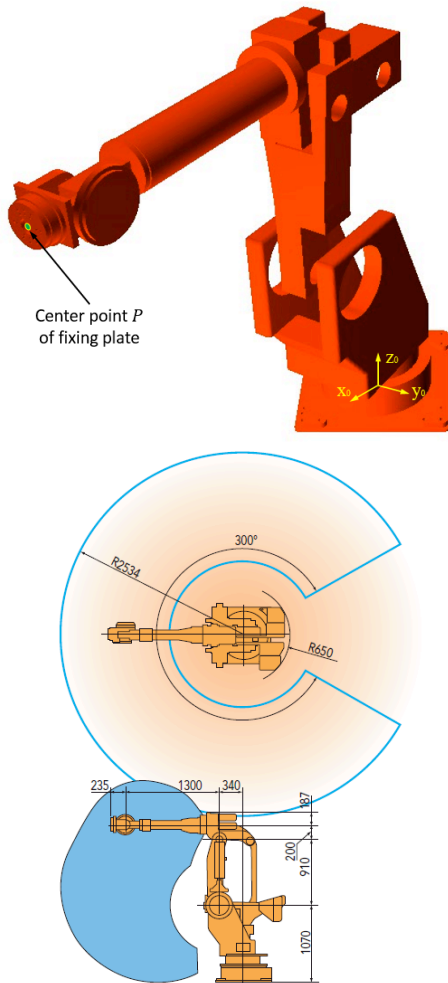
Figure 1: Working envelop and links schematic of Nachi Robot (SC300F-02).

The sixth link carrying the operation point P is connected to the base frame through a serial chain composed of six-revolute joints. The kinematic chain of Nachi Robot (SC300F-02) is shown in Figure **2**.
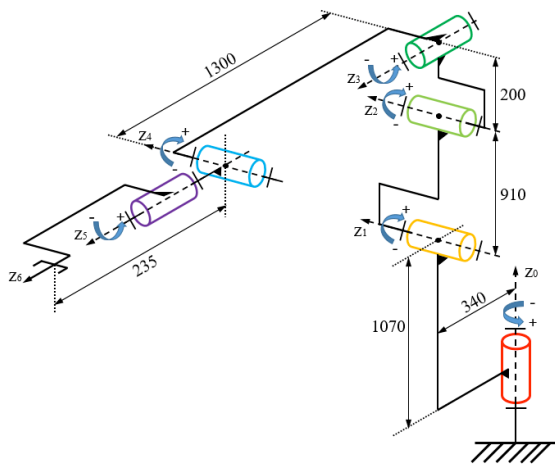
But one thing needs to be noticed is that at current posture, the joints value displayed on the robot's touchpad is $\begin{bmatrix} 0° & 90° & 0° & 0° & 0° & 0° \end{bmatrix}$. In order to build a D-H model could represent the real robot perfectly, all of the joint value should be set to $0°$, thus the robot's posture will be look like as the Figure **3**:
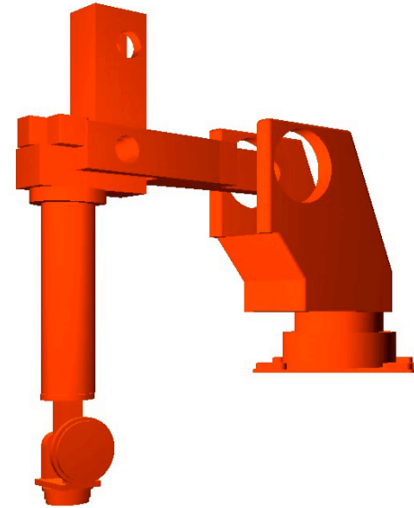

Figure 3: Robot's posture when joints value as $\begin{bmatrix} 0° & 0° & 0° & 0° & 0° & 0° \end{bmatrix}$.

Start at joint 1, z_0 represents the first joint, which is the base revolute joint, x_0 is chosen to be the same direction as the reference frame x-axis of the robot controller, this is done for convenience to verify the correctness of the D-H model. x_0 is a fixed field axis, it represents the base of the robot. Next, z_1 is assigned at joint 2. x_1 will be normal to z_0 and z_1, because these two axes are intersecting. x_2 will be in the direction of the common normal between z_1 and z_2. x_3 is in the

Figure 2: Kinematic chain schematic of Nachi Robot (SC300F-02).
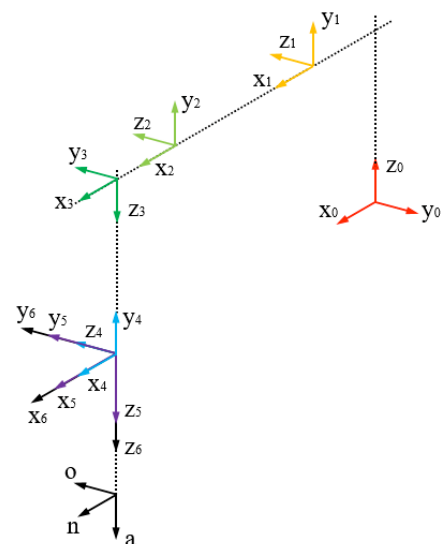

Figure 4: Reference frames representation of Nachi robot.

direction of the common normal between z_2 and z_3. In order to ensure the solvability of the inverse kinematic of robot, z_4, z_5 and z_6 are assigned at the same origin point. Normally, the end effector is not included in the equations of motions, but it can be represented by an additional line in the D-H parameters table. In the case, the tip point of end effector physically represents the center point of the fixing plate of the joint 6, it is also as the same as the coordinate value that indicated on the robot's touch pad.

According to these assigned coordinate frames, the parameters of D-H model can be filled out in Table **1**. Notice that the rotations are measured with the right-hand rule. The curled fingers of your right hand, rotating in the direction of rotation, determine the direction of the axis of rotation along the thumb.

Table 1: D-H Model Parameters of Nachi Robot (SC300F-02)

i	θ_i	d_i	a_i	α_i
1	θ_1	1070	340	90
2	θ_2	0	910	0
3	θ_3	0	200	90
4	θ_4	1300	0	-90
5	θ_5	0	0	90
6	θ_6	0	0	0
Tool	0	235	0	0

T_n represents the transformation matrix of end effector frame relative to the base frame of a n degree of freedom series robot. The position and orientation of an arbitrary point $^n p = \begin{bmatrix} p_x & p_y & p_z \end{bmatrix}$ on the end effector can be described in the robot base coordinates frame as following:

$$^0 p = T_n {}^n p = A_1 A_2 A_3 \cdots A_n {}^n p \tag{9}$$

For a robot which structure has been determined, according to D-H model table, link length a_i, link off set d_i, and link rotation angle α_i are all known parameters, θ_i are the variables changing with the movement of the robot. Thus, the equations of forward kinematic can be written as:

$$T_n = A_1(\theta_1) A_2(\theta_2) A_3(\theta_3) \cdots A_n(\theta_n) \tag{10}$$

For the Nachi robot, there are 6 joints, the transformation between each two successive joints can be written by simply substituting the parameters from the Table **1**:

$$A_1 = \begin{bmatrix} C_1 & 0 & S_1 & a_1 C_1 \\ S_1 & 0 & -C_1 & a_1 S_1 \\ 0 & 1 & 0 & d_1 \\ 0 & 0 & 0 & 1 \end{bmatrix} \tag{11}$$

$$A_2 = \begin{bmatrix} C_2 & -S_2 & 0 & a_2 C_2 \\ S_2 & C_2 & 0 & a_2 S_2 \\ 0 & 0 & 1 & 0 \\ 0 & 0 & 0 & 1 \end{bmatrix} \tag{12}$$

$$A_3 = \begin{bmatrix} C_3 & 0 & S_3 & a_3 C_3 \\ S_3 & 0 & -C_3 & a_3 S_3 \\ 0 & 1 & 0 & 0 \\ 0 & 0 & 0 & 1 \end{bmatrix} \tag{13}$$

$$A_4 = \begin{bmatrix} C_4 & 0 & -S_4 & 0 \\ S_4 & 0 & C_4 & 0 \\ 0 & -1 & 0 & d_4 \\ 0 & 0 & 0 & 1 \end{bmatrix} \tag{14}$$

$$A_5 = \begin{bmatrix} C_5 & 0 & S_5 & 0 \\ S_5 & 0 & -C_5 & 0 \\ 0 & 1 & 0 & 0 \\ 0 & 0 & 0 & 1 \end{bmatrix} \tag{15}$$

$$A_6 = \begin{bmatrix} C_6 & -S_6 & 0 & 0 \\ S_6 & C_6 & 0 & 0 \\ 0 & 0 & 1 & 0 \\ 0 & 0 & 0 & 1 \end{bmatrix} \tag{16}$$

In the equations, S_i represents $\sin(\theta_i)$, C_i represents $\cos(\theta_i)$.

T_6 is a 4×4 homogeneous matrix, the forward kinematic solution of Nachi Robot it can be written as following:

$$T_6 = \begin{bmatrix} n_x & o_x & a_x & p_x \\ n_y & o_y & a_y & p_y \\ n_z & o_z & a_z & p_z \\ 0 & 0 & 0 & 1 \end{bmatrix} = A_1 A_2 A_3 A_4 A_5 A_6 \tag{17}$$

Or it can be written in a lite form:

$$T_6 = \begin{bmatrix} \bar{n} & \bar{o} & \bar{a} & \bar{p} \\ 0 & 0 & 0 & 1 \end{bmatrix} = A_1 A_2 A_3 A_4 A_5 A_6 \tag{18}$$

Each element in the Jacobian is the derivative of a corresponding kinematic equation with respect to one of the variables. Referring to Equation (2.8), the first element in $\dot{x}$ is dx. This means the first kinematic equation must represent movements along the x-axis, which, of course, would be p_x. In other words, p_x

expresses the motion of the hand frame along the x-axis, and thus, its derivative will be *dx*. The same will be true for *dy* and *dz*. Considering the $\bar{n}$, $\bar{o}$, $\bar{a}$, $\bar{p}$ matrix, the corresponding elements of p_x, p_y, p_z can be picked and be differentiated to get the *dx*, *dy* and *dz*. However, since there is no unique equation that describe the rotations about the axes, thus there is no single equation available for differential rotations about the three axes, namely, δx, δy and δz. As a result, these have to be calculated differently.

Actually, it is a lot simpler to calculate the Jacobian relative to T_6, the last frame, than it is to calculate it relative to the first frame. The velocity equation relative to the last frame can be written as:

$$^{T_6}\dot{x} = {}^{T_6}J(q)\dot{q} \tag{19}$$

$^{T_6}\dot{x}$ is the vector representing the position and orientation of robot's end effector in last frame, $\dot{q}$ is the vector representing the angle value of each joint. This means that for the same joint differential motions, pre-multiplied with the Jacobian matrix relative to the last frame, the operation point differential motions relative to the last frame can be obtained. One can calculate the Jacobian with respect to the last frame using following formation steps:

(1)   The differential motion relationship of equation can be written as

$$
\begin{bmatrix} {}^{T_6}dx \\ {}^{T_6}dy \\ {}^{T_6}dz \\ {}^{T_6}\delta x \\ {}^{T_6}\delta y \\ {}^{T_6}\delta z \end{bmatrix} =
\begin{bmatrix}
{}^{T_6}J_{11} & {}^{T_6}J_{12} & \cdots & {}^{T_6}J_{16} \\
{}^{T_6}J_{21} & {}^{T_6}J_{22} & \cdots & {}^{T_6}J_{26} \\
{}^{T_6}J_{31} & {}^{T_6}J_{32} & \cdots & {}^{T_6}J_{36} \\
{}^{T_6}J_{41} & {}^{T_6}J_{42} & \cdots & {}^{T_6}J_{46} \\
{}^{T_6}J_{51} & {}^{T_6}J_{52} & \cdots & {}^{T_6}J_{56} \\
{}^{T_6}J_{61} & {}^{T_6}J_{62} & \cdots & {}^{T_6}J_{66}
\end{bmatrix}
\begin{bmatrix} d\theta_1 \\ d\theta_2 \\ d\theta_3 \\ d\theta_4 \\ d\theta_5 \\ d\theta_6 \end{bmatrix} \tag{20}
$$

(2)   Assuming that any combination of $A_1, A_2, ...A_n$ can be expressed with a corresponding $\bar{n}, \bar{o}, \bar{a}, \bar{p}$ matrix, the corresponding elements of the matrix will be used to calculate the Jacobian.

(3)   If joint *i* under consideration is a revolute joint, then:

$$
\begin{bmatrix} {}^{T_6}J_{1i} \\ {}^{T_6}J_{2i} \\ {}^{T_6}J_{3i} \\ {}^{T_6}J_{4i} \\ {}^{T_6}J_{5i} \\ {}^{T_6}J_{6i} \end{bmatrix} =
\begin{bmatrix} (-n_x p_y + n_y p_x) \\ (-o_x p_y + o_y p_x) \\ (-a_x p_y + a_y p_x) \\ n_z \\ o_z \\ a_z \end{bmatrix} \tag{21}
$$

(4)   The column *i* use $^{i-1}T_6$:

For column 1, use $^0T_6 = A_1 A_2 A_3 A_4 A_5 A_6$

For column 2, use $^1T_6 = A_2 A_3 A_4 A_5 A_6$

For column 3, use $^2T_6 = A_3 A_4 A_5 A_6$

For column 4, use $^3T_6 = A_4 A_5 A_6$

For column 5, use $^4T_6 = A_5 A_6$

For column 6, use $^5T_6 = A_6$

4. FORCE JACOBIAN MATRIX OF ROBOT

When an external load applied on the robot end effector, if the robot system is in equilibrium state, the driving force generated by each joint should be balance with the external load. The external load can be written as $F = [f, n]^T$, so called the generalized end effector force vector. Revolute joint provides driving torque, prismatic joint provide drive force. For the Nachi Robot, the driving torques provided by the six revolute joints are $\tau_1, \tau_2, ... \tau_6$, these can be written as:

$$\tau = \begin{bmatrix} \tau_1 & \tau_2 & \tau_3 & \tau_4 & \tau_5 & \tau_6 \end{bmatrix}^T \tag{22}$$

So called the generalized joint force vector.

According to the principle of virtual work, make the virtual displacement of each joint is *dq*, the virtual displacement of end effector is *dX*, thus the sum of virtual work by each joint force is:

$$W_q = \tau^T dq = \tau_1 dq_1 + \tau_2 dq_2 \cdots + \tau_6 dq_6 \tag{23}$$

The virtual work by end effector force is:

$$W_F = F^T dX \tag{24}$$

According to the sum of virtual work should be zero, thus:

$$\tau^T dq = F^T dX \tag{25}$$

From Equation (2.1), there is:

$$dX = J(q)dq \tag{26}$$

From Equation (3.4) and (3.5), there is:

$$\tau^T dq = F^T J(q) dq$$
$$\Rightarrow \tau = J^T(q) F \tag{27}$$

$J^T(q)$ is force Jacobian matrix of robot, when the robot system is in equilibrium state, it represents the mapping relationship between external load and joint force. It is also the transposed matrix of Jacobian matrix.

5. CARTESIAN STIFFNESS MATRIX FORMULATION OF ROBOT SYSTEM

The robot system stiffness refers to the ability of resist to deformation, especially the displacement of end effector, when robot subjected to external robot. Make external load as $F = \begin{bmatrix} fx & fy & fz & nx & ny & nz \end{bmatrix}^T$, the tiny displacement of end effector subjected to external load is $dX = \begin{bmatrix} dx & dy & dz & \delta x & \delta y & \delta z \end{bmatrix}^T$. When displacement is small enough, there are linear relationship between these two: *F=KdX*. It can be written in matrix form:

$$\begin{bmatrix} f_x \\ f_y \\ f_z \\ n_x \\ n_y \\ n_z \end{bmatrix} = \begin{bmatrix} k_{11} & k_{12} & \cdots & k_{16} \\ k_{21} & k_{22} & \cdots & k_{26} \\ k_{31} & k_{32} & \cdots & k_{36} \\ k_{41} & k_{42} & \cdots & k_{46} \\ k_{51} & k_{52} & \cdots & k_{56} \\ k_{61} & k_{62} & \cdots & k_{66} \end{bmatrix} \begin{bmatrix} d\theta_1 \\ d\theta_2 \\ d\theta_3 \\ d\theta_4 \\ d\theta_5 \\ d\theta_6 \end{bmatrix} \tag{28}$$

F is the external load applied on end effector relative to the base coordinate frame of robot, it contains the force and torque in three degrees of freedom. *dX* is the displacement of the end effector relative the base coordinate of robot, it contains the translation and rotation in three degrees of freedom. Both of these are 6-dimensinal vectors. *K* is 6×6 matrix, it is the cartesian stiffness matrix of robot system.

The cartesian stiffness matrix of robot system depends on robot's configuration, link stiffness, control loop stiffness and the actuators' mechanical stiffness. For the slim and long structure, like the repair manipulator applied in space station, the deformation of link is the main factor that affect the robot stiffness. The components of transmission system, like the gears, belt and shaft, will be deformed under driving force. Especially, when the transmission line is long, these deformations could be accumulated and coupling with each other.

Because the deformation and stiffness properties are distributed in the robot system, and the statistical data shows that 70% or higher of deformation is come from the insufficient stiffness of driving and transmission system for the industrial robot. Thus,

assume the deformation concentrate on the joints is reasonable. In this paper, the links of robot are assumed to be rigid, the damping is neglected and the stiffness of the joints is represented with the linear torsional springs, the coefficient of elasticity is k_{qi}, so called the joint stiffness, as shown in Figure **5**. The reciprocal of k_{qi} is C_{qi}, so called the flexibility. For a 6 DOF robot, k_q is the diagonal joint stiffness matrix defined as follows:

$$K_q = \begin{bmatrix} k_{q1} & 0 & 0 & 0 & 0 & 0 \\ 0 & k_{q2} & 0 & 0 & 0 & 0 \\ 0 & 0 & k_{q3} & 0 & 0 & 0 \\ 0 & 0 & 0 & k_{q4} & 0 & 0 \\ 0 & 0 & 0 & 0 & k_{q5} & 0 \\ 0 & 0 & 0 & 0 & 0 & k_{q6} \end{bmatrix} \tag{29}$$
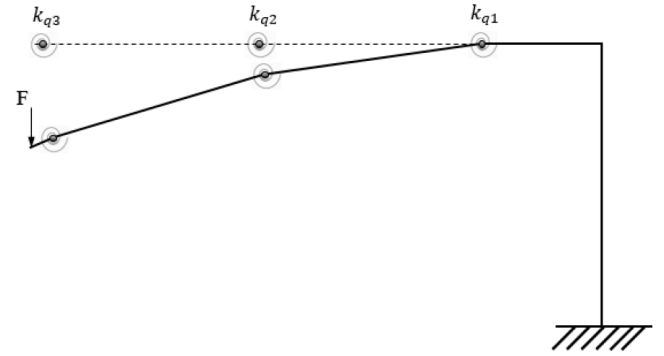

Figure 5: A 3-DOF robot model with linear torsional springs as joints.

For a *n* DOF robot, assume the stiffness of each joint is $k_{qi}(i=1,2,...,n)$, the displacement of end effector is *dX* which subject to the external load *F*, the angle changing of each joint is $d_{qi}(i=1,2,...,n)$, there is:

$$\tau_i = k_{qi}d_{qi}(i=1,2,...,n) \tag{30}$$

τ_i is torque on each joint, it is due to the elastic deformation of the robot system.

This can be written in matrix form as:

$$\tau = K_q d_q \tag{31}$$

In the above equation, $d_q = \begin{bmatrix} d_{q1} & d_{q1} ... d_{qn} \end{bmatrix}^T$, $K_q = diga\begin{bmatrix} k_{q1}, & k_{q2}, ..., k_{qn} \end{bmatrix}$.

Make the robot system stiffness equivalent to each joint, the mapping relationship between joints stiffness and end effector stiffness can be established, the derivation process as following:

From the jacobian matrix of robot, there is:

$$dX = J(q)dq \qquad (32)$$

From the force jacobian matrix of robot, there is:

$$\tau = J^T(q)F \qquad (33)$$

From equation (3.10) and equation (3.12), there is:

$$K_q d_q = J^T(q)F$$
$$\Rightarrow d_q = k_q^{-1} J^T(q)F \qquad (34)$$

From equation (3.11) and equation (3.13), there is:

$$dX = J(q)K_q^{-1}J^T(q)F \qquad (35)$$

Make $C(q) = J(q)K_q^{-1}J^T(q)$, thus:

$$dX = C(q)F \qquad (36)$$

$C(q)$ is flexibility matrix of end effector.

Equation (3.14) pre-multiplied by $J^{-1}(q), Kq$ and $J^{-T}(q)$ Successively;

$$\Rightarrow J^{-1}(q)dX = J^{-1}(q)J(q)K_q^{-1}J^T(q)F$$

$$\Rightarrow J^{-1}(q)dX = K_q^{-1}J^T(q)F$$

$$\Rightarrow K_q J^{-1}(q)dX = K_q K_q^{-1}J^T(q)F$$

$$\Rightarrow K_q J^{-1}(q)dX = J^T(q)F$$

$$\Rightarrow J^{-T}(q)K_q J^{-1}(q)dX = J^{-T}(q)J^T(q)F$$

$$\Rightarrow J^{-T}(q)K_q J^{-1}(q)dX = J^{-T}(q)J^T(q)F$$

$$\Rightarrow J^{-T}(q)K_q J^{-1}(q)dX = F$$

Make,

$$K(q) = J^{-T}(q)\,K_q J^{-1}(q) \qquad (37)$$

Thus:

$$F = K(q)dX \qquad (38)$$

$K(q) = J^{-T}(q)\,K_q J^{-1}(q)$ is the end effector stiffness matrix, derivation is completed.

The stiffness matrix $K(q)$ or flexibility matrix $C(q)$ represents the linear relationship between the external load applied on end effector and the displacement of end effector, and these matrixes change with the changing of robot's position and orientation. As can be seen from the elements in stiffness matrix, the force of one direction not only cause the deformation on this direction, but also cause the deformation in other directions. For example, the diagonal element k_{22} in stiffness matrix represents the f_y caused by d_y on y direction, the non-diagonal element k_{62} in stiffness matrix represents the n_z caused by d_y on z direction.

6. ROBOT TRAJECTORY STIFFNESS EVALUATION FORMULATION

The zigzag path is a typical trajectory for robotic hybrid manufacturing as shown in Figure **6**. One layer of this kind path could work for machining or milling process, multiple layers of that could be used as a deposition working path. When robot carry the deposition extruder or machining tools moving along the straight line segments, the operation speed usually is set at a constant value, the robot system is in equilibrium state. But when the robot moves to the
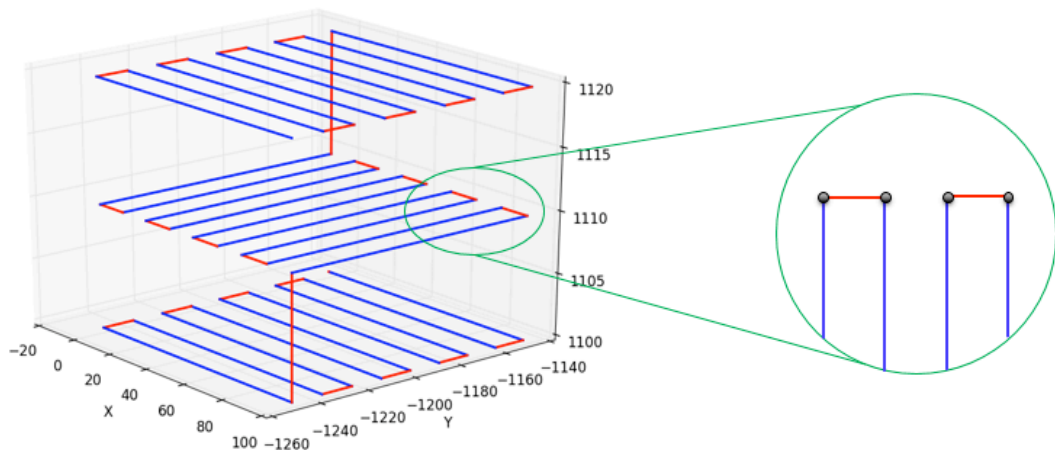

Figure 6: Zigzag path for hybrid manufacturing and turning points in the trajectory.

turning points in the trajectory, the end effector often accompanied with intensely changing of acceleration in different directions. The initial cutting force or inertia of heavy deposition equipment in directions of acceleration changing will cause unbalanced force on the robot system, so the robot demands higher stiffness property at these turning points positions.

As mentioned in the previous section, the robot joint stiffness matrix K_q is a diagonal matrix, so $K_q = K_q^T$, simultaneous this with equation (3.17), there is:

$$K(q) = K(q)^T \tag{39}$$

This is the symmetry property of $K(q)$, which is $k_{ij} = k_{ji}$, it illustrates that if the force in j direction can cause a unit deformation in i direction, then the same force in i direction can cause a unit deformation in j direction. The non-diagonal elements in $K(q)$ represents the coupling relationship between the force and displacement in different direction. When the non-diagonal element equal 0, which means there is no coupling relationship between these two directions. For example, when there is no coupling relationship between the force and displacement in x and y direction, then there is $k_{12} = k_{21} = 0$.

In addition, $K(q)$ is a positive-definite matrix, simultaneous with it symmetry property, the diagonal elements and the principal minor determinant of each order are more than 0, this can be written as:

$$k_{ii} > 0, \det\left(\begin{bmatrix} k_{11} & \cdots & k_{1i} \\ \vdots & \ddots & \vdots \\ k_{i1} & \cdots & k_{ii} \end{bmatrix}\right) > 0, i = 1, 2, \cdots, 6 \tag{40}$$

According to the analysis of $K(q)$'s properties, and notice that the stiffness matrix is changing when robot at different position and orientation, an evaluation formulation can be created to illustrate the difference of trajectory's stiffness performance at different position and orientation within robot working envelop:

$$E = \sum_{i=1}^{6} k_{ii} + \sum_{i=1, j=1, i \neq j}^{6} |k_{ij}| \tag{41}$$

7. SIMULATION: STIFFNESS MAPPING OF A ROBOTIC HYBRID MANUFACTURING WORKING PATH

The initial motivation of applying robot in hybrid manufacturing is overcome the building size limitation of conventional CNC machines. Figure **7** show a schematic of the fused pellets deposition (FPM)

extruder installed on the Nachi robot, this equipment can realize deposit large scale part in a relatively short period. But the weight of the FPM extruder is over 500lb, this is an external load cannot be ignored during operation. Thus it is necessary use trajectory stiffness evaluation method to help planning the working path.
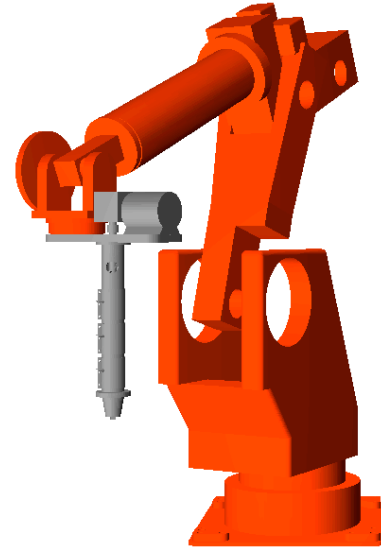

Figure 7: Assembly model of FPM system.

For conducting a specific working path, there are multiple choices of position and orientation in the robot working envelop. Based on the robot kinematic and stiffness evaluation formulation, a trajectory stiffness evaluation simulation system can be programmed with Python, the flow chart of this simulation analysis system as shown in Figure **8**.
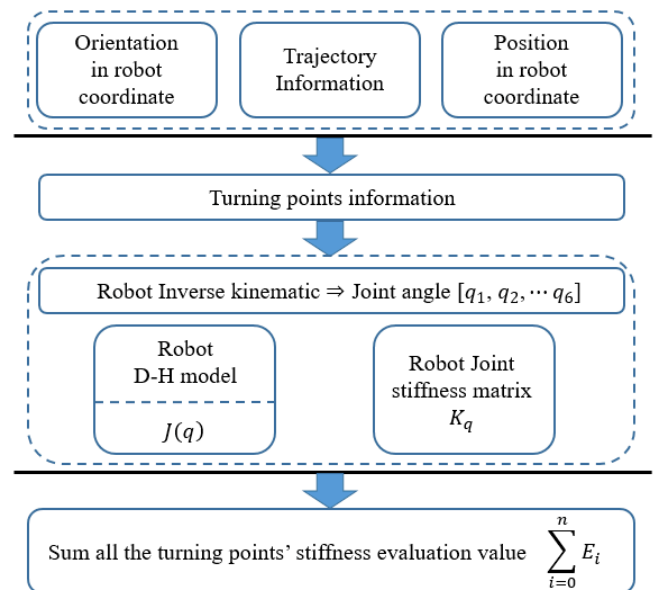

Figure 8: Flow chart of trajectory stiffness evaluation simulation system.
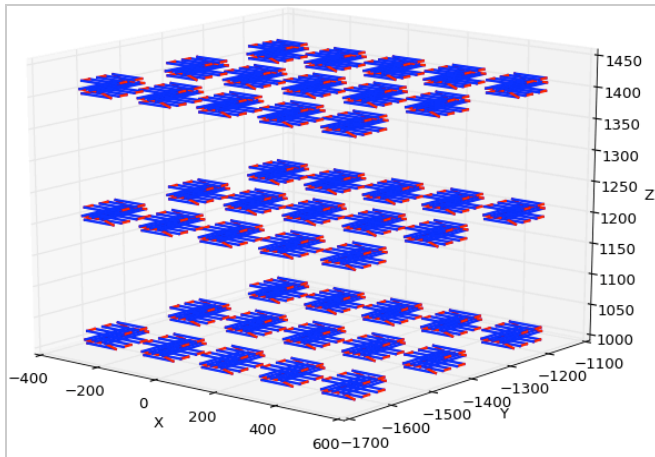
Figure 9: Trajectory testing cube within robot working envelop.

In order to study how zigzag trajectory's position and orientation affect its stiffness in the working envelop of robot, firstly separate working volume into small testing cube area $(200mm \times 200mm \times 200mm)$ within the x range is from -500 to 500, y range is from -1200 to -1800, z range is from 800 to 1400, in robot system coordinate. The dimension of deposition zigzag path is $100mm \times 100mm \times 30mm$, layer thickness is 10mm, track width is 20mm and overlap is 0.3, thus there are 45 testing cube areas within robot working envelop, as shown in Figure **9**.

Secondly, set the orientation angle for these trajectories, start from x-axis positive direction, rotate about z-axis counterclockwise, take the angle value as $0°, 60°, 120°, 180°, 240°, 300°$, respectively. Then apply the trajectory stiffness analysis process to these zigzag

Table 2: $100mm \times 100mm \times 300mm$ Trajectory Stiffness Evaluation Value

| Trajectory position index	Rotation angle (°)											
	0		60		120		180		240		300	
	Value	Rank	Value	Rank	Value	Rank	Value	Rank	Value	Rank	Value	Rank
1	57912008.5	16	57917201.5	16	58023086.2	16	58098883.1	16	57982785.1	16	57899655.5	16
2	62189826.6	25	62177482.3	25	62238753.2	25	62319313.1	25	62268150.5	25	62198579.2	25
3	63186832.3	27	63162031.7	27	63192306.8	27	63266548.0	27	63256148.0	27	63205920.5	27
4	53285991.7	4	53299057.5	4	53384377.6	4	53404272.6	4	53305523.2	4	53271486.8	4
5	57421016.3	15	57417061.0	15	57472652.6	15	57516140.2	15	57461913.1	15	57421446.2	15
6	59000277.0	19	58983756.3	19	59015254.4	19	59065204.6	19	59044628.4	19	59010565.4	19
7	51508067.0	1	51522248.2	1	51579577.2	1	51567781.9	1	51500388.5	1	51497801.0	1
8	54659692.6	9	54659664.5	9	54702410.9	9	54719810.0	9	54675017.5	9	54657182.4	9
9	56152074.0	12	56140577.0	12	56167441.0	12	56197837.4	12	56176134.9	12	56156830.7	12
10	51419211.9	0	51430333.4	0	51460867.5	0	51440559.1	0	51400559.1	0	51413793.8	0
11	53368017.0	5	53368650.2	5	53396299.6	5	53398184.2	5	53367248.3	5	53364656.5	5
12	54440081.0	8	54430997.9	8	54450115.7	8	54466352.4	8	54448439.6	8	54441096.0	8
13	52164260.4	2	52170766.7	2	52180043.9	2	52155719.1	2	52142697.5	2	52161140.1	2
14	53076982.5	3	53076309.6	3	53089746.1	3	53083921.4	3	53065778.1	3	53072425.1	3
15	53645742.1	6	53637095.4	6	53647414.2	6	53654094.2	6	53641445.7	6	53643383.3	6
16	73443909.7	36	73420000.6	36	73535555.1	36	73692566.6	36	73596953.9	36	73460405.2	36
17	75636443.9	38	75604032.5	38	75668940.1	38	75780194.8	38	75778766.6	38	75677509.0	38
18	74860829.0	37	74820718.6	37	74855339.6	37	74966442.1	37	74978485.2	37	74906726.1	37
19	64402023.5	30	64396711.1	30	64503089.4	30	64581091.8	30	64482815.3	30	64408016.5	30
20	67652769.3	32	67635441.2	32	67700507.0	32	67786708.7	32	67746833.8	32	67676755.0	32
21	68235388.9	33	68208558.4	33	68247052.8	33	68328566.8	33	68321784.0	33	68266431.5	33
22	59097087.6	20	59103493.5	20	59183625.6	20	59213191.8	20	59140921.2	20	59104406.8	20
23	62120889.2	24	62113648.6	24	62169417.0	24	62221092.2	24	62181115.1	24	62136012.4	24
24	63232961.1	28	63215517.6	28	63251622.0	28	63308565.0	28	63293570.5	28	63253606.0	28
25	56080975.2	10	56091933.9	10	56144625.0	10	56153200.0	10	56108066.5	10	56088833.8	10
26	58451823.2	17	58450434.4	17	58493031.0	17	58522436.0	17	58489623.2	17	58461390.3	17
27	59627644.9	21	59616398.3	21	59646464.4	21	59684707.5	21	59667856.7	21	59640602.8	21
28	54333450.4	7	54344378.4	7	54376489.0	7	54378560.4	7	54350578.5	7	54338064.0	7
29	56118242.9	11	56119624.4	11	56149451.5	11	56165633.1	11	56140196.4	11	56122657.9	11
30	57175331.2	14	57167859.3	14	57190380.5	14	57215016.1	14	57190026.8	14	57181766.9	14
31	88574068.5	44	88529787.1	44	88619540.6	44	88828436.1	44	88813640.6	44	88646634.4	44
32	87420580.4	43	87375345.4	43	87435825.8	43	87596780.7	43	87616362.0	43	87499901.4	43
33	84942871.8	42	84893153.4	42	84932478.4	42	85066465.9	42	85099371.8	42	85014684.8	42
34	75849792.0	39	75826520.5	39	75925689.9	39	76065664.0	39	76009206.7	39	75890040.7	39
35	77035187.2	41	77008058.1	41	77072891.5	41	77193342.4	41	77182329.7	41	77088091.5	41
36	76425986.6	40	76392257.0	40	76435917.5	40	76541272.0	40	76550420.2	40	76478337.4	40
37	66838747.2	31	66833073.6	31	66922348.9	31	67005968.4	31	66945252.7	31	66866016.8	31
38	69042978.1	34	69029348.6	34	69091190.3	34	69176008.0	34	69150092.0	34	69078205.8	34
39	69575120.6	35	69553403.0	35	69596732.2	35	69676568.7	35	69670665.6	35	69612149.6	35
40	60648881.9	23	60654519.9	23	60725155.0	23	60774268.8	23	60722885.2	23	60667777.9	23
41	63113367.5	26	63109194.0	26	63163058.5	26	63220357.6	26	63189754.8	26	63136220.4	26
42	64250581.8	29	64237617.3	29	64277140.7	29	64335566.6	29	64321325.6	29	64275581.9	29
43	56424502.0	13	56435653.5	13	56489190.8	13	56518331.5	13	56475400.1	13	56435091.1	13
44	58856879.1	18	58858784.4	18	58902798.7	18	58940188.8	18	58909419.9	18	58869947.2	18
45	60270174.0	22	60263350.3	22	60296984.2	22	60338155.3	22	60319812.4	22	60285295.1	22
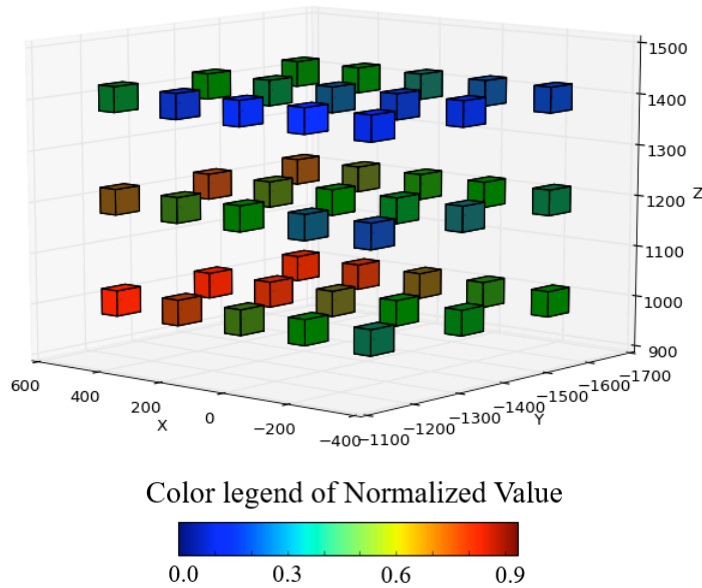
Figure 10: Trajectory stiffness mapping results for small scale working path.

trajectories which at different positions and with different orientations, the results are shown in Table **2**.

As can be seen from Table **1**, for the same angle group, the position affects the trajectory stiffness obviously. But for the same position with different angle, the evaluation result is close, take the maximum value position 31 as example, the difference between max and min is only 0.37%. Moreover, the rank of evaluation result in different angle group is the same. This leads to the stiffness trajectory mapping result is the identical for these 6 groups, as shown in Figure **10**. The color of cube is assigned as the normalized evaluation values. The higher of the evaluation result is, the better stiffness can be obtained at this position. So the best position to perform this task is at the center point of [500, -1200, 1000].

The reason of this result is the size of the deposition part. The stiffness property of robot is distributed unevenly within its working envelop, the larger of the

task's operation range, the more different stiffness area the robot will cross. For the small scale working path, in macro view, most turning points are concentrated within a small area, even with the changing of working path's orientation, the gesture of robot manipulator did not change a lot. Thereby, it is more meaningful to discuss how the orientation affect a large scale working path's stiffness performance, this is also the initial goal of applying robot in hybrid manufacturing.

Take a large size deposition task as example, the dimension of deposition zigzag path is $800mm \times 800mm \times 500mm$, layer thickness is 10mm, track width is 20mm and overlap is 0.3, thus there is only one center point option for this trajectory: [0, -1600, 800]. Then set the orientation angle for these trajectories, start from x-axis positive direction, rotate about z-axis counterclockwise, take the angle value as $0°, 60°, 120°, 180°, 240°, 300°$, respectively. The stiffness evaluation result for this task is shown in Figure **11**.
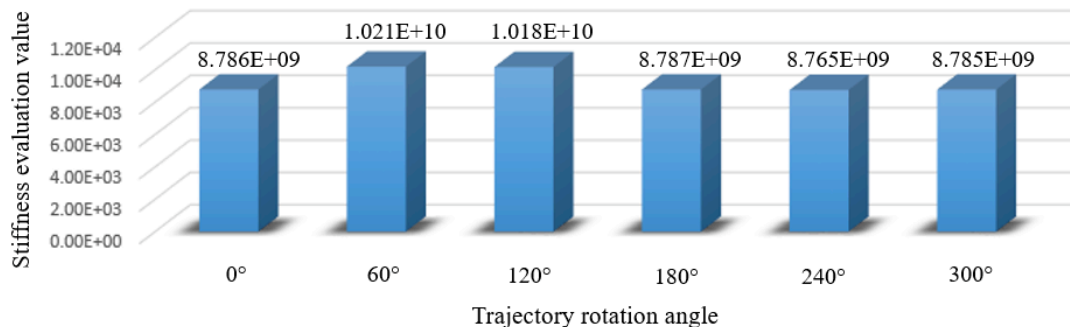

Figure 11: Trajectory stiffness mapping results for large scale working path.

The difference between maximum value and minimum value is 14%, much more obvious than the small size working path. The higher of the evaluation result is, the better stiffness can be obtained at this orientation. So the best orientation to perform this task is 60°.

CONCLUSION

The subject of this paper was to develop a new methodology for finding the best position and orientation to perform heavy duty tasks based on the current robot system stiffness capability. Firstly, the definition of jacobian matrix was introduced, and the Nachi Robot (SC300F-02) was used as an illustrate example throughout this paper. The detail process of solving robot jacobian matrix was presented, and the force jacobian matrix also has been derived according to the concept of virtual work. Based the on the assumptions of the link of industrial robot is rigid and all the deformation are concentrated at joints, the stiffness model of serial manipulator was developed. Then the robot stiffness matrix was derived from the robot jacobian matrix and robot joint stiffness matrix. By analyzing the robot kinematic and the properties of robot stiffness matrix, a new evaluation formulation has been established for mapping the trajectory's stiffness within the robot's working volumetric. A trajectory stiffness simulation analysis system was developed for discussing the stiffness difference of a robotic deposition working path at different positions and orientations. The simulation results revealed that for the small size working path, in macro view, most turning points are concentrated within a small area, position is the main factor that affect the stiffness performance of this specific task. But for the large scale working path, the orientation of trajectory would affect the distribution of turning pointing a lot, thus lead to a great difference of stiffness performance. Moreover, this method not only benefits the application of using robot in hybrid manufacturing process, it is also important for improving the operation performance when robot is applied in other heavy duty task situation.

ACKNOWLEDGEMENTS

REFERENCE

[1]   Zha and Xuan F. Optimal pose trajectory planning for robot manipulators. Mechanism and Machine Theory 2002; 37(10): 1063-1086.
http://dx.doi.org/10.1016/S0094-114X(02)00053-8

[2]   Kim, Taejung, and Sanjay E. Sarma. Toolpath generation along directions of maximum kinematic performance; a first cut at machine-optimal paths. Computer-Aided Design 2002; 34.6: 453-468.
http://dx.doi.org/10.1016/S0010-4485(01)00116-6

[3]   Schneider, Ulrich, *et al*. Combining holistic programming with kinematic parameter optimisation for robot machining. ISR/Robotik 2014; 41st International Symposium on Robotics; Proceedings of VDE 2014.

[4]   Urbanic RJ, Hedrick R and Ana M. Djuric. A Linkage Based Solution Approach for Determining 6 Axis Serial Robotic Travel Path Feasibility. SAE International Journal of Materials and Manufacturing 2016; 0336: 444-456.

[5]   Matsuoka, Shin-ichi, *et al*. High-speed end milling of an articulated robot and its characteristics. Journal of materials processing technology 1999; 95.1: 83-89.

[6]   Pan, Zengxi, *et al*. Chatter analysis of robotic machining process. Journal of materials processing technology 2006; 173.3: 301-309.
http://dx.doi.org/10.1016/j.jmatprotec.2005.11.033

[7]   Wang, Guifeng, *et al*. Dynamic cutting force modeling and experimental study of industrial robotic boring. The International Journal of Advanced Manufacturing Technology 2015: 1-12.

[8]   Mekaouche, Adel, Frédéric Chapelle and Xavier Balandraud. FEM-based generation of stiffness maps. IEEE Transactions on Robotics 2015; 31.1: 217-222.
http://dx.doi.org/10.1109/TRO.2015.2392351

[9]   Zhang, Pu, Zhenqiang Yao and Zhengchun Du. Global performance index system for kinematic optimization of robotic mechanism. Journal of Mechanical Design 2014; 136.3: 031001.

[10] Nawratil Georg. New performance indices for 6R robots. Mechanism and machine theory 2007; 42.11: 1499-1511.
http://dx.doi.org/10.1016/j.mechmachtheory.2006.12.007

[11] Olds and Kevin C. Global Indices for kinematic and force transmission performance in parallel robots. IEEE Transactions on Robotics 2015; 31.2: 494-500.
http://dx.doi.org/10.1109/TRO.2015.2398632

[12] Mansouri I and Ouali M. A new homogeneous manipulability measure of robot manipulators, based on power concept. Mechatronics 2009; 19.6: 927-944.
http://dx.doi.org/10.1016/j.mechatronics.2009.06.008

[13] Chen, Yonghua and Fenghua Dong. Robot machining: recent development and future research issues. The International Journal of Advanced Manufacturing Technology 2013; 66.9-12: 1489-1497.

[14] Guérin, David, *et al*. Optimal measurement pose selection for joint stiffness identification of an industrial robot mounted on a rail. 2014 IEEE/ASME International Conference on Advanced Intelligent Mechatronics. IEEE, 2014.
http://dx.doi.org/10.1109/AIM.2014.6878332

[15] Klimchik, Alexandr, *et al*. Accuracy improvement of robot-based milling using an enhanced manipulator model. Advances on Theory and Practice of Robots and Manipulators. Springer International Publishing 2014; 73-81.

[16] Abele E, Weigold M and Rothenbücher S. Modeling and identification of an industrial robot for machining applications.

CIRP Annals-Manufacturing Technology 2007; 56.1: 387-390.
http://dx.doi.org/10.1016/j.cirp.2007.05.090

[17] Moosavian, Amin and Fengfeng Jeff Xi. Design and analysis of reconfigurable parallel robots with enhanced stiffness. Mechanism and Machine Theory 2014; 77: 92-110.
http://dx.doi.org/10.1016/j.mechmachtheory.2014.02.005

[18] Robin, Vincent, Laurent Sabourin and Grigore Gogu. Optimization of a robotized cell with redundant architecture. Robotics and Computer-Integrated Manufacturing 2011; 27.1: 13-21.
http://dx.doi.org/10.1016/j.rcim.2010.06.010

[19] Pitt E. Bryn, Nabil Simaan and Eric J. Barth. An Investigation of Stiffness Modulation Limits in a Pneumatically Actuated Parallel Robot with Actuation Redundancy. ASME/BATH

2015 Symposium on Fluid Power and Motion Control. American Society of Mechanical Engineers 2015.

[20] Gosselin and Clement. Stiffness mapping for parallel manipulators. Robotics and Automation, IEEE Transactions on 1990; 6.3: 377-382.

[21] Majou, Félix, *et al*. Parametric stiffness analysis of the Orthoglide. Mechanism and Machine Theory 2007; 42.3: 296-311.
http://dx.doi.org/10.1016/j.mechmachtheory.2006.03.018

[22] Ruggiu and Maurizio. Cartesian stiffness matrix mapping of a translational parallel mechanism with elastic joints. International Journal of Advanced Robotic Systems 2012; 9.

[23] Pinto, Charles, *et al*. A methodology for static stiffness mapping in lower mobility parallel manipulators with decoupled motions. Robotica 2010; 28.05: 719-735.
http://dx.doi.org/10.1017/S0263574709990403